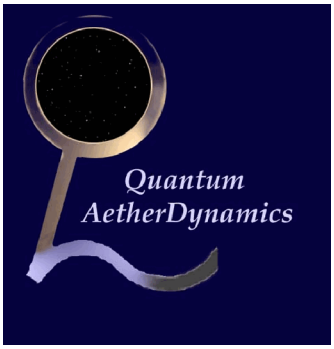

Quantum AetherDynamics Institute (QADI)

Recruitment-Energy Tests for Collective Aether Cells: Boundary Penalties, Phase Costs, and Source Consistency

David W. Thomson III
Quantum AetherDynamics Institute (QADI), Alma, Illinois, USA
ORCID: 0000-0002-5830-5427
DOI: 10.5281/zenodo.22103229

Version 1.1 – October 18, 2026

This article is published by the Quantum AetherDynamics Institute (QADI).

It develops the Aether Physics Model (APM)

Abstract

The collective Aether-cell construction supplies density-compatible coherence branches, but its gravitational source and recruitment mechanism require an interaction energy. This paper tests proposed energies against the source and same-density transition conditions established in Paper II. Four reciprocal conductance–flux mismatch potentials have zero value and zero first derivative on the registration constraint; any smooth finite multiple of these penalties therefore supplies neither a bulk interaction source nor a preference among registered branches. The von Mises phase law remains a useful statistical representation, but its diverging concentration parameter is not itself a mechanical energy. If either the concentration parameter or its Legendre rate function is assigned a fixed positive cold-energy amplitude, the interaction pressure diverges at saturation and the corresponding sound response exceeds any finite causal limit near that endpoint, assuming a finite smooth baseline.

Two bounded alternatives illustrate the additional requirements. Branch-independent linear alignment and quadratic coherence costs fail simultaneous energy and pressure matching. Their branch coefficients and offsets can be constrained to match both quantities, but the matched quadratic example favors the enlarged branch before the proposed saturation boundary. A matched affine alignment family has the required local ordering at the first three tested transitions and gives explicit constraints on the baseline equation of state and interaction amplitude. These are conditional energetic completions, not microscopic derivations: their absolute amplitude, reference energy, and baseline stiffness remain independent inputs. Reproducible calculations isolate which proposed terms can contribute to the neutron-to-gravity source problem and which additional physics is still required.

Keywords: Quantum Measurement Units; Aether Physics Model; collective Aether cells; neutron matter; recruitment energy; gravitational source; thermodynamic matching; phase coherence

1 Question and scope

Paper II separates three tasks: density registration, branch selection, and thermodynamic completion Thomson [2026]. Registration fixes the coherence compatible with a chosen contributor count and neutron density. It does not specify the energy carried by that state, its pressure, or which contributor count minimizes the energy. The present contribution is to apply the resulting source and transition tests to explicit energy candidates.

The analysis concerns a local, homogeneous, zero-temperature sector at fixed neutron fraction. There are no gradient, surface, kinetic, or external-reservoir terms. A common baseline matter energy is retained separately. The transition test concerns continuous switching at the *same density*, with no latent energy. A first-order transition with different coexistence densities would require a separate analysis. None of the tests below constitutes a neutron-star solution or a microscopic derivation of an Aether interaction.

The earlier version characterized the fixed-branch phase singularity and a reciprocal boundary minimum as microscopic closure. The present tests replace that inference with a sharper result: a boundary minimum can enforce matching without providing a bulk source, and an infinite statistical parameter does not by itself establish an infinite physical cost. The useful phase identities are retained, while the energetic conclusions are stated only for declared energy assignments.

2 Geometry, source, and transition requirements

2.1 Collective geometry and its response

For an even contributor count $M = 2K$, define

$$F_{M,q}(x) = 1 + 2\sum_{k=1}^{M-1}\left(1 - \frac{k}{M}\right) q^k \cos(kx), \tag{1}$$

$$D_M(q) = \frac{1}{L_0}\int_0^\pi \sqrt{1 + 4\sin^2\theta\, F_{M,q}(2\theta)^2}\,\mathrm{d}\theta, \tag{2}$$

$$L_0 = \int_0^\pi \sqrt{1 + 4\sin^2\theta}\,\mathrm{d}\theta = 5.27036716319126. \tag{3}$$

The registration constraint is

$$D_M(q) = (n_{\mathrm{n}} V_0)^{-1/3}, \qquad n_{\mathrm{n}} = Y_{\mathrm{n}} n_{\mathrm{B}}. \tag{4}$$

The supplied reference volume is $V_0 = 2.483401334974\,\mathrm{fm}^3$; it is an input to the density translation, not a prediction or an exact measured constant. Its uncertainty is not supplied. On a decreasing branch,

$$\chi_M(q) = -\frac{D_M}{3D_{M,q}} > 0, \qquad \frac{\mathrm{d}q}{\mathrm{d}\ln n_{\mathrm{B}}} = \chi_M(q), \qquad \chi_{M,q} = -\frac{1}{3} + \frac{D_M D_{M,qq}}{3D_{M,q}^2}. \tag{5}$$

Every use of the endpoint below assumes a finite nonzero negative $D_{M,q}(1)$. This is checked for the finite ranks used numerically; no all-rank monotonicity theorem is inferred from a grid.

The proposed saturation rule admits $M + 2$ when the old branch reaches $q = 1$ and imposes

$$D_{M+2}(q_{\mathrm{e}}) = D_M(1). \tag{6}$$

This rule remains a model postulate until a microscopic mechanism selects it. In particular, the enlarged branch is already geometrically admissible at lower densities.

2.2 QMU energy and gravitational source

Use the QMU energy and pressure scales Thomson [2025]

$$E_{\mathrm{q}} = \mathrm{angm} F_q = m_e \lambda_C^2 F_q^2, \qquad P_{\mathrm{q}} = \frac{E_{\mathrm{q}}}{\lambda_C^3}, \qquad \nu_{\mathrm{B}} = n_{\mathrm{B}}\lambda_C^3. \tag{7}$$

The conversion identity $c = \lambda_C F_q$ gives $E_{\mathrm{q}} = m_e c^2$. A declared dimensionless interaction energy per baryon u gives

$$\epsilon_{\mathrm{A}} = E_{\mathrm{q}} n_{\mathrm{B}} u, \qquad p_{\mathrm{A}} = E_{\mathrm{q}} n_{\mathrm{B}}\left(\nu_{\mathrm{B}} u_{\nu_{\mathrm{B}}} + \chi_M u_q\right). \tag{8}$$

Partial derivatives hold the other arguments fixed. For $u = u_M(q)$, introduce

$$P_M = \frac{p_{\mathrm{A}}}{E_{\mathrm{q}} n_{\mathrm{B}}} = \chi_M u_{M,q}, \qquad C_M = \frac{\mathrm{d}^2 u_M}{\mathrm{d}(\ln n_{\mathrm{B}})^2} = \chi_M \chi_{M,q} u_{M,q} + \chi_M^2 u_{M,qq}. \tag{9}$$

These follow by varying the energy *along* the registration constraint, rather than holding q fixed. The cold-fluid variational framework is discussed by Brown Brown [1993].

The comoving mass contribution is $\rho_{\mathrm{A}} = \epsilon_{\mathrm{A}}/c^2$. In the Aether mass ledger with mass unit m_a,

$$\widehat{\rho}_{\mathrm{A}} = \frac{m_e}{m_a}\nu_{\mathrm{B}} u. \tag{10}$$

For a perfect-fluid sector moving with Lorentz factor W relative to the normal observer, its measured energy density is $(\epsilon_{\mathrm{A}} + p_{\mathrm{A}})W^2 - p_{\mathrm{A}}$. Consequently, neither a conductance coordinate nor a dimensionless mismatch penalty becomes a gravitational source until an energy law is supplied. If u depends on composition only through q, the additional consistency identity is

$$Y_{\mathrm{n}} \left(\frac{\partial \epsilon_{\mathrm{A}}}{\partial Y_{\mathrm{n}}}\right)_{n_{\mathrm{B}},M} = p_{\mathrm{A}}. \tag{11}$$

This identity does not impose chemical equilibrium; it states the composition response of the assumed sector.

2.3 Junction and bulk stability tests

At a same-density junction with a common branch-independent baseline and no latent, surface, or reservoir term, Paper II requires

$$u_M(1) = u_{M+2}(q_{\mathrm{e}}), \qquad \chi_M(1)u_{M,q}(1) = \chi_{M+2}(q_{\mathrm{e}})u_{M+2,q}(q_{\mathrm{e}}). \tag{12}$$

Both energy and pressure must match. The sector chemical potential is $E_{\mathrm{q}}(u + P)$, so it matches as well. Offsets can repair the first condition, but cannot repair the second.

Write the total energy as $\epsilon = E_{\mathrm{q}} n_{\mathrm{B}} f$, with $f = f_{\mathrm{b}}(n_{\mathrm{B}}) + u_M(q(n_{\mathrm{B}}))$ at fixed composition. Let $z = \ln(n_{\mathrm{B}}/n_{\mathrm{B}}^{\mathrm{ref}})$, $P_{\mathrm{b}} = \mathrm{d}f_{\mathrm{b}}/\mathrm{d}z$, and $C_{\mathrm{b}} = \mathrm{d}^2 f_{\mathrm{b}}/\mathrm{d}z^2$. Then

$$\frac{\mu}{E_{\mathrm{q}}} = f + P_{\mathrm{b}} + P_M, \qquad \frac{c_s^2}{c^2} = \frac{P_{\mathrm{b}} + C_{\mathrm{b}} + P_M + C_M}{f + P_{\mathrm{b}} + P_M}. \tag{13}$$

Admissibility requires a positive denominator and, for a stable causal local fluid, a ratio between zero and one. These conditions apply to the *total* energy. Negative binding energy or negative interaction pressure alone does not decide stability.

At fixed density, energetic branch selection additionally compares u_{M+2} with u_M wherever both exist. Smooth matching does not imply that the old branch is energetically preferred up to its endpoint.

3 Reciprocal boundary penalties are source-null on registration

The QMU conductance–flux representation takes the normalized boundary variables as $C_{\mathrm{A}}/\mathrm{cond} = D$ and $\mathrm{mflx}_{\mathrm{A}}/\mathrm{mflx} = D^{-1}$, with $\mathrm{mflx} = \mathrm{cond}^{-1}$. A natural mismatch coordinate is $r = D_{\mathrm{new}}/D_{\mathrm{ref}} > 0$. The four proposed penalties are

$$V_1(r) = \tfrac{1}{4}(r - r^{-1})^2, \qquad V_2(r) = (\ln r)^2, \tag{14}$$

$$V_3(r) = \tfrac{1}{2}(r + r^{-1} - 2), \qquad V_4(r) = \tfrac{1}{2}\left[(r-1)^2 + (r^{-1} - 1)^2\right]. \tag{15}$$

Each has a unique minimum at $r = 1$, and

$$V_i(1) = V_i'(1) = 0, \qquad (V_1'', V_2'', V_3'', V_4'')(1) = (2, 2, 1, 2). \tag{16}$$

Theorem 3.1 (Source-null penalty)**.** *Let $u_{\mathrm{pen}} = \lambda(\nu_{\mathrm{B}}, Y_{\mathrm{n}}, M, q)V(r)$, where λ is smooth and finite and $V(1) = V'(1) = 0$. If registration enforces $r = 1$, then this penalty contributes zero energy density, zero pressure, and zero first composition response on the registered states. If all admitted branches use the same zero-minimum construction, the penalty alone gives no energetic preference among them.*

Proof. On $r = 1$, $u_{\mathrm{pen}} = 0$. Every first derivative is a sum of terms proportional to $V(1)$ or $V'(1)$ and therefore vanishes. Substitution into Eq. (8) proves the source statement, and comparison of the identical branch values proves the selection statement. □

There are two distinct uses of the reference. If $D_{\mathrm{ref}} = D_{\mathrm{cell}}(n_{\mathrm{B}}, Y_{\mathrm{n}})$, the penalty vanishes along every registered branch. If $D_{\mathrm{ref}} = D_M(1)$ is held fixed, the new-branch penalty vanishes at the junction only. In the latter case it still cannot repair a nonzero bulk energy or pressure mismatch at that junction. Adding such a penalty to a separate bulk energy leaves the bulk matching residuals unchanged.

The nonzero second derivative does provide an off-constraint stiffness,

$$u_{\mathrm{pen},qq}\big|_{r=1} = \lambda V''(1) \left(\frac{D_{\mathrm{new},q}}{D_{\mathrm{ref}}} \right)^2, \tag{17}$$

but its magnitude depends on the unspecified physical amplitude. A dynamical relaxation rate also needs a kinetic or dissipative law. Gradient or interface contributions lie outside this local theorem.

Reciprocity alone does not select the matched state. For example,

$$V_*(r) = (r + r^{-1} - 5/2)^2 \tag{18}$$

is nonnegative and reciprocal, yet has minima at $r = 2$ and $r = 1/2$, while $V_*(1) = 1/4$. A minimum at unity requires an additional assumption about the functional, beyond reciprocal coordinates.

4 Phase statistics and conditional singular energy assignments

4.1 What the phase singularity establishes

For the von Mises nearest-neighbor phase distribution,

$$p_\kappa(\Delta) = \frac{e^{\kappa \cos \Delta}}{2\pi I_0(\kappa)}, \qquad q = \langle \cos \Delta \rangle = \frac{I_1(\kappa)}{I_0(\kappa)}, \tag{19}$$

the Bessel identities and large-argument expansions National Institute of Standards and Technology give

$$\frac{\mathrm{d}q}{\mathrm{d}\kappa} = 1 - q^2 - \frac{q}{\kappa}, \qquad \delta \equiv 1 - q \sim \frac{1}{2\kappa}, \qquad \frac{\mathrm{d}q}{\mathrm{d}\kappa} \sim 2\delta^2. \tag{20}$$

The derivative at $\kappa = 0$ is its limit $1/2$. Thus $q \to 1$ requires $\kappa \to \infty$ within this statistical family. The geometrical coordinate satisfies

$$\kappa[D_M(q) - D_M(1)] \longrightarrow \frac{|D_{M,q}(1)|}{2}. \tag{21}$$

For $n_{\mathrm{n}}(q) = 1/[V_0 D_M(q)^3]$, likewise

$$\kappa[n_{\mathrm{n}}(1) - n_{\mathrm{n}}(q)] \longrightarrow \frac{3n_{\mathrm{n}}(1)|D_{M,q}(1)|}{2D_M(1)}. \tag{22}$$

These are valid changes of statistical coordinate, not energy balances.

In particular, a microscopic phase Hamiltonian $H = -\mathcal{J}\cos\Delta$ with finite coupling $\mathcal{J}$ would give $\kappa = \mathcal{J}/(k_{\mathrm{B}}T)$ in a canonical ensemble. Its $T \to 0$ limit has $\kappa \to \infty$ and finite mean energy $-\mathcal{J}q \to -\mathcal{J}$. This example demonstrates why the divergence of κ does not by itself force recruitment. It is not a derivation of $\mathcal{J}$ or of a cold Aether Hamiltonian.

4.2 Two explicit cold-energy hypotheses

Define the dimensionless Legendre rate function relative to the uniform phase distribution,

$$J(q) = \kappa(q)q - \ln I_0(\kappa(q)), \qquad J_q = \kappa, \qquad J(q) \sim \tfrac{1}{2}\ln(\pi/\delta) - \tfrac{1}{2}. \tag{23}$$

It is a statistical information cost. Its conversion into a physical energy or free energy requires a scale and a thermodynamic interpretation. A temperature-dependent free energy is not automatically the cold energy in Eq. (8).

Theorem 4.1 (Failure of fixed positive singular costs at saturation)**.** *Consider either $u = a\kappa(q) + b$ or $u = aJ(q) + b$, with fixed $a > 0$ and finite b. Assume D_M is smooth near $q = 1$, $D_{M,q}(1) < 0$, a finite endpoint density, and a common baseline with finite energy and first two z derivatives there. Then neither assignment reaches $q = 1$ with finite interaction energy and pressure. The total cold sound response also becomes unbounded and positive near that endpoint.*

Proof. Set $\chi_* \equiv \chi_M(1) > 0$. For the concentration cost,

$$u \sim \frac{a}{2\delta}, \quad P_M \sim \frac{a\chi_*}{2\delta^2}, \quad C_M \sim \frac{a\chi_*^2}{\delta^3}, \quad \frac{c_s^2}{c^2} \sim \frac{2\chi_*}{\delta}. \tag{24}$$

For the rate-function cost,

$$u \sim \frac{a}{2}\ln(\pi/\delta), \quad P_M \sim \frac{a\chi_*}{2\delta}, \quad C_M \sim \frac{a\chi_*^2}{2\delta^2}, \quad \frac{c_s^2}{c^2} \sim \frac{\chi_*}{\delta}. \tag{25}$$

The finite baseline cannot cancel these leading terms in Eq. (13). All stated divergences follow as $\delta \to 0^+$. □

This exclusion concerns fixed positive cold-energy assignments, the specified saturation endpoint, and the stated local domain. It does not exclude the phase probability law, finite-energy alignment models, transitions at $q < 1$, amplitudes that vanish near the endpoint, or a different coupled energy sector. Such modifications require their own source and matching tests. A finite new-branch energy at $q_{\mathrm{e}} < 1$ cannot smoothly match an infinite old-branch energy or pressure using finite offsets.

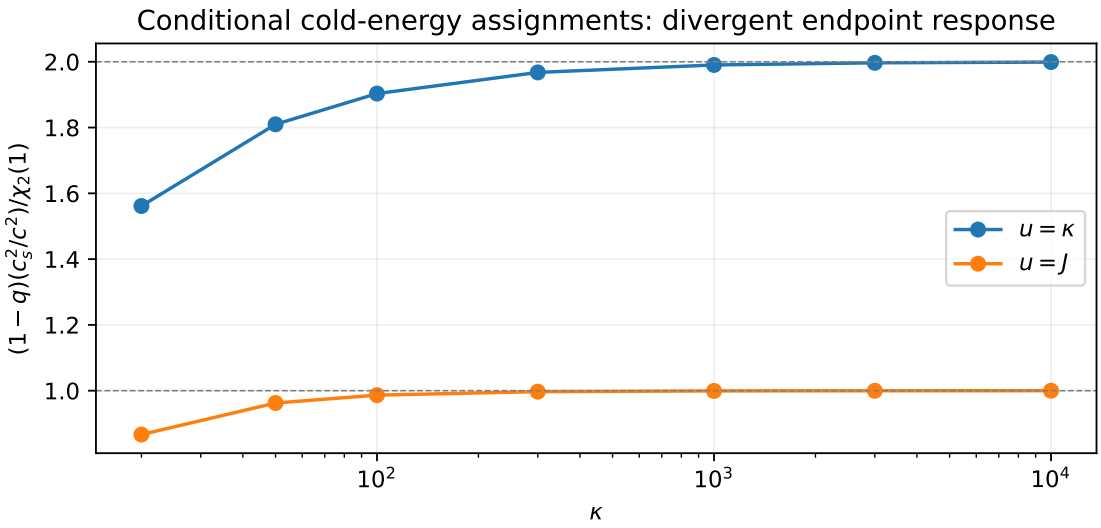

Figure 1: Numerical check of the two singular-cost asymptotics on $M = 2$. The normalized sound response tends to 2 for $u = \kappa$ and to 1 for $u = J$. Unit amplitudes and a finite constant baseline $f_b = 1$ are diagnostic normalizations, not a matter EOS. The unnormalized sound response diverges.

5 Bounded energies: matching is necessary but insufficient

5.1 General coefficient and offset conditions

Test the bounded diagnostic family

$$u_M(q) = a_M f(q) + b_M. \tag{26}$$

Neither the shape, coefficients, nor offsets are derived here from microscopic Aether dynamics. If the derivatives in the denominator are nonzero, Eq. (12) requires

$$\frac{a_{M+2}}{a_M} = \frac{\chi_M(1) f'(1)}{\chi_{M+2}(q_e) f'(q_e)}, \tag{27}$$

$$b_{M+2} = b_M + a_M f(1) - a_{M+2} f(q_e). \tag{28}$$

The offsets are energy contributions, not merely dispensable conventions. A common change of energy zero must be compensated in the baseline to preserve the gravitational source. Relative offsets between branches are physical recruitment energies in this model.

For a bounded alignment cost $f(q) = 1 - q$, the pressure is $P_M = -a_M \chi_M$. At a common positive amplitude and zero offsets, the old energy is zero at saturation, whereas the new energy is $a_M(1 - q_e) > 0$; pressures also differ. For a quadratic coherence cost $f(q) = q^2$, the new-minus-old energy is $a_M(q_e^2 - 1) < 0$ and the pressure mismatch is $2a_M[\chi_{M+2}(q_e)q_e - \chi_M(1)]$. Neither common-amplitude model passes both junction conditions.

Simple common normalizations do not provide these ratios. At the first transition, constant, total nearest-neighbor-link, and link-per-contributor factors $g_M = 1$, $M - 1$, and $(M - 1)/M$ give new-to-old factors 1, 3, and 1.5. These are only illustrative counts. A microscopic theory would still need

Transition	q_e	$\chi_M(1)$	$\chi_{M+2}(q_e)$	Alignment ratio	Quadratic ratio
$2 \to 4$	.50189564	10.747684	.87390083	12.298517	24.504133
$4 \to 6$	.78372969	6.615615	.89867846	7.361492	9.392897
$6 \to 8$	.87453142	5.877667	.96115765	6.115196	6.992540

Table 1: Required coefficient ratios a_{M+2}/a_M from pressure matching for two diagnostic shapes. The values depend on the collective geometry, not on the density-unit conversion or an EOS fit. Last digits are numerical, not physical precision.

to identify which links carry energy and convert their number to energy per baryon; a link count alone does not establish the needed coefficient.

5.2 A local test of branch ordering

Let $\Delta u(z) = u_{M+2}(q_{M+2}(z)) - u_M(q_M(z))$ at the same density. If both matching conditions hold at z_j, then

$$\Delta u(z_j) = \Delta u_z(z_j) = 0, \qquad \Delta u(z) = \tfrac{1}{2}\Delta C_j (z - z_j)^2 + o((z - z_j)^2). \tag{29}$$

Thus $\Delta C_j < 0$ means that the enlarged branch is favored already just below the proposed endpoint. Energy and pressure matching alone do not prevent premature recruitment.

Normalize the old coefficient to $a_M = 1$ and its offset to zero separately at each junction. For the first transition, the matched alignment example requires

$$a_4 = 12.2985172676, \qquad b_4 = -6.1259450797, \qquad \Delta C_j = +2232.922598. \tag{30}$$

It therefore has the required *local* preference for the old branch. The matched quadratic example requires

$$a_4 = 24.5041325361, \qquad b_4 = -5.1725721879, \qquad \Delta C_j = -4659.442897. \tag{31}$$

It fails that ordering test despite exact energy and pressure matching. For example, at $n_n/n_{n,j} = 0.99$, the normalized gaps are about $+0.0415641$ for alignment and -0.0856406 for the quadratic model.

The curvature signs persist at the next two tested junctions. For $4 \to 6$, ΔC_j is approximately $+1574.7083$ for alignment and -3221.7774 for the quadratic model. The supplied script evaluates 401 densities over each pair's common geometrically admissible interval for all three transitions. All sampled gaps have the corresponding signs, up to endpoint roundoff. These samples supplement the analytic local criterion; they are not a global proof for all ranks or all possible energy shapes.

6 A conditional affine completion and its source bounds

6.1 Matching determines relative branch coefficients

The bounded alignment family can be written

$$u_M(q) = u_* + \gamma v_M(q), \qquad v_M(q) = A_M - B_M q, \qquad \gamma > 0. \tag{32}$$

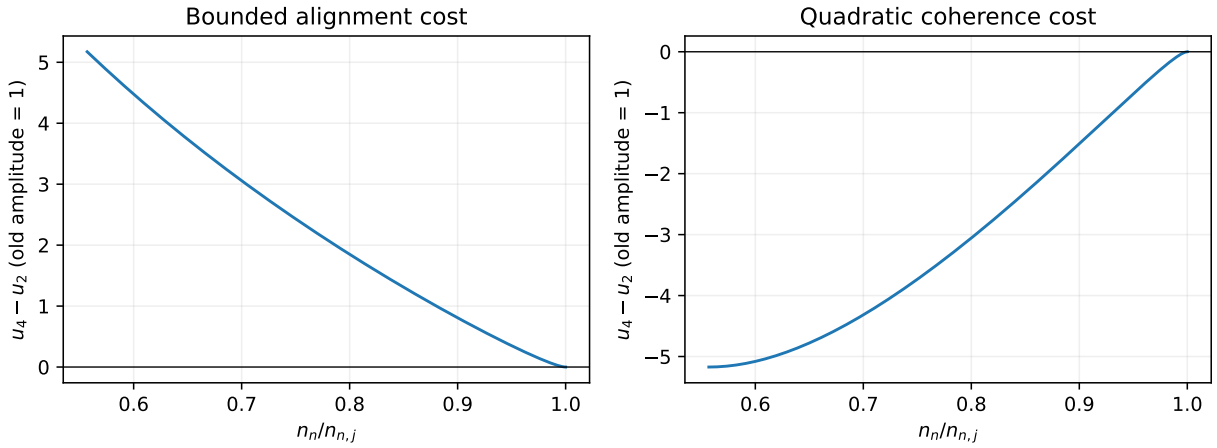

Figure 2: First-transition energy gaps after matching both energy and pressure. Positive gap favors the old $M = 2$ branch; negative gap favors $M = 4$. Each panel uses its own old-amplitude normalization. The quadratic example favors the enlarged branch before saturation, whereas the bounded alignment example has the intended ordering over the sampled interval.

M	A_M	B_M	$v_M(1)$
2	0	1	−1
4	5.172572	12.298517	−7.125945
6	63.829367	90.535439	−26.706073
8	457.471185	553.641923	−96.170738
10	2671.238561	3019.427902	−348.189341
12	13878.623593	15138.295781	−1259.672188

Table 2: Conditional affine coefficients, with $A_2 = 0$ and $B_2 = 1$. Their substantial finite-rank growth makes the absolute amplitude and baseline constraints consequential. No asymptotic growth law is claimed from this finite table.

Set $A_2 = 0$, $B_2 = 1$ as a dimensionless reference and keep the common energy u_* explicit. Matching imposes

$$B_{M+2} = B_M \frac{\chi_M(1)}{\chi_{M+2}(q_e)}, \qquad A_{M+2} = A_M - B_M + B_{M+2} q_e. \tag{33}$$

These relations specify the relative coefficients once the branch sequence is assumed. They do not determine γ, u_*, or the baseline matter energy. In particular, they do not predict an absolute gravitational source.

The sector source is now explicit, conditional on those inputs:

$$\widehat{\rho}_A = \frac{m_e}{m_a} \nu_B [u_* + \gamma(A_M - B_M q)], \qquad \frac{p_A}{P_q} = -\nu_B \gamma B_M \chi_M. \tag{34}$$

This identifies precisely what a microscopic calculation must supply to turn density registration into an independently normalized source.

6.2 Baseline stiffness and amplitude inequalities

Absorb the common u_* into f_b when testing the total EOS. Define

$$H_\mathrm{b} = f_\mathrm{b} + P_\mathrm{b}, \qquad N_\mathrm{b} = P_\mathrm{b} + C_\mathrm{b}, \tag{35}$$

$$H_v = v_M - B_M\chi_M, \qquad N_v = -B_M\chi_M(1+\chi_{M,q}). \tag{36}$$

The complete local stability and causal conditions are

$$H_\mathrm{b} + \gamma H_v > 0, \qquad 0 \le N_\mathrm{b} + \gamma N_v \le H_\mathrm{b} + \gamma H_v. \tag{37}$$

Where $H_v < 0$ and $N_v < 0$, necessary pointwise amplitude bounds include

$$\gamma < \frac{H_\mathrm{b}}{-H_v}, \qquad \gamma \le \frac{N_\mathrm{b}}{-N_v}, \qquad \gamma(N_v - H_v) \le H_\mathrm{b} - N_\mathrm{b}. \tag{38}$$

The last inequality should be applied with its displayed sign; division requires checking the sign of $N_v - H_v$. The allowed amplitude must satisfy the bounds over every state in the intended domain and on both sides of each junction.

For example, on the old side of the first transition the normalized affine family gives

$$H_v = -11.74768448, \qquad N_v = -2246.42929809. \tag{39}$$

Thus positive chemical potential requires $H_\mathrm{b} > 11.74768448\gamma$, and nonnegative compressibility requires $N_\mathrm{b} \ge 2246.42929809\gamma$ at that point, in addition to the upper sound-speed bound. These are quantitative requirements on a future baseline calculation, not a fitted amplitude or a prediction of its size.

For a constant rest-energy baseline, $N_\mathrm{b} = 0$. Wherever $N_v < 0$, any positive γ then gives negative compressibility. A rest-energy offset can help the chemical-potential denominator but cannot supply the missing stiffness. A positive-pressure, sufficiently stiff baseline or another derived interaction term is therefore required. The data file reports H_v and N_v at the tested branch endpoints so that a specified baseline can be assessed without repeating the geometry calculation.

The affine family passes the finite source and junction tests and the demonstrated local branch-order tests. Its *total* thermodynamic admissibility remains conditional on Eq. (37). It also provides no nucleation barrier, relaxation time, or microscopic rule for admitting the next intact cell. Those require an actual dynamical model.

7 Results and requirements for microscopic completion

The strongest contribution is a set of exclusion and completion conditions, together with a nontrivial bounded candidate that survives some of them. The common conductance–flux boundary is useful as a registration condition. It does not determine the source. The phase law is useful as a coherence coordinate. It does not determine the recruitment work. Even a matched source law must be checked for premature branch preference and total compressibility.

A microscopic completion must derive an energy per baryon, identify which degrees of freedom carry it, specify its absolute normalization and reference relative to the matter sector, and reproduce

Candidate	Result within the stated domain
Reciprocal mismatch penalties	Source-null on registration; cannot alone select among registered branches or repair a bulk junction mismatch.
Fixed positive $a\kappa$ or aJ	Divergent energy, pressure, and cold sound response at the proposed $q = 1$ endpoint.
Common-amplitude bounded costs	Finite, but fail simultaneous energy and pressure matching.
Matched quadratic cost	Satisfies both junction equalities, but favors the enlarged branch prematurely near the first three tested endpoints.
Matched affine alignment	Finite and matched, with the intended local ordering at the first three tested endpoints; needs an independent energy scale, reference contribution, and a baseline satisfying the total-EOS bounds.

Table 3: Energy tests distinguish geometric matching from a gravitational source and from energetic branch selection.

both sides of Eq. (12). It must then establish the energetically selected branch sequence and satisfy Eq. (37) over its stated density and composition domain. A future mechanism may change the saturation rule rather than reproduce it. The tests here provide concrete criteria for deciding that question without calibrating a putative interaction energy to gravitational observations.

A Numerical reproduction and limits

The package contains a standalone Python script, requirements, CSV tables, JSON validation summary, and the figures used here. The deformation and its first two q derivatives use 640-point Gauss–Legendre quadrature. Independent adaptive quadrature checks selected ranks through $M = 24$, and finite differences check the second derivative and constrained pressure. Sixty-digit Bessel calculations prevent cancellation in the small phase susceptibility. The singular-cost normalization uses $a = 1$ and a finite constant baseline solely to verify the analytic endpoint limits.

The branch-gap comparison samples 401 densities in each pair's common geometrically admissible interval for $2 \to 4$, $4 \to 6$, and $6 \to 8$. Local signs at the junction also follow from the evaluated curvature formula in Eq. (29); the samples do not prove global branch selection or stability for an infinite hierarchy. Recursive affine coefficients are tabulated through $M = 24$ as a finite audit. No EOS dataset, stellar mass, radius, tidal observable, or measured gravitational constant is used to fix an energy amplitude.

Density translations inherit the reference-volume assumption. The dimensionless matching ratios, source-null theorem, and singular-cost asymptotics do not depend on the conversion from reference volume to fm^{-3}. The retained DOI is the manuscript's supplied identifier; this package is a revision for review and does not assert that a new version has already been deposited.

References

J. David Brown. Action functionals for relativistic perfect fluids. *Classical and Quantum Gravity*, 10(8):1579–1606, 1993. doi: 10.1088/0264-9381/10/8/017.

National Institute of Standards and Technology. Digital Library of Mathematical Functions: Modified Bessel Functions. URL https://dlmf.nist.gov/10. Sections 10.29 and 10.40; accessed October 18, 2026.

David W. Thomson, III. Reference Tables for Quantum Measurement Unit (QMU) Conversions: CGS and MKS Systems, 2025. URL https://doi.org/10.5281/zenodo.17683574.

David W. Thomson, III. Collective Aether-Cell Coherence and the Neutron-to-Gravity Source Problem: Geometric Bounds, Branch Selection, and Thermodynamic Completion, 2026. URL https://doi.org/10.5281/zenodo.22102013. Companion manuscript revision, version 1.3, October 18, 2026; supplied record DOI.